Available online at www.sciencedirect.com
SCIENCE DIRECT
Sensors and Actuators B 111–112 (2005) 84–90
SENSORS AND ACTUATORS B CHEMICAL
www.elsevier.com/locate/snb

"NO-selective" NO_x sensing elements for combustion exhausts

David L. West *, Fred C. Montgomery, Timothy R. Armstrong

Metals and Ceramics Division, Oak Ridge National Laboratory, Building 4508, MS 6083, Oak Ridge, TN 37831 6083, USA

Available online 3 August 2005

Abstract

Fabrication and characterization of NO_x sensing elements using co-planar oxide and Pt electrodes is described. The sensing elements, based on yttria-stabilized zirconia substrates, could be current-biased to a "NO-selective" sensing condition (for NO_x in the concentration range 50–1500 ppm_V) if the oxide was an alkaline earth-modified lanthanum chromite. Simple variations in electrode geometry (interdigitation of the electrodes or increase of the oxide electrode surface area relative to the Pt electrode) did not affect the magnitude of the NO response or the recovery from exposure to NO. The main effects of temperature appeared to be a decrease in the response magnitude with increasing *T* and an increase of the recovery time (from NO exposure) with decreasing *T*.

Keywords: NO_x sensor; Nitric oxide; Gas sensor

1. Introduction

The three main pollutants (excluding CO_2) in combustion exhausts from low-sulfur fuels are carbon monoxide (CO), hydrocarbons (HC), and oxides of nitrogen (NO_x, a mixture of NO and NO_2). Currently, for the exhausts from fuel-injected, spark-ignited engines, a three-way catalyst (TWC) is employed that greatly reduces the levels of all three pollutants (CO, HC, and NO_x). The TWC is only effective within a narrow range of O_2 concentrations in the exhaust [1], losing its effectiveness for NO_x removal at higher [O_2]. Therefore, the presently used TWC cannot be employed for NO_x remediation of exhausts from diesel and lean-burn gasoline engines, as these tend to be O_2-rich.

If a suitable "lean NO_x" catalyst is not developed, diesel and lean-burn gasoline exhausts will require on-board NO_x remediation with techniques such as selective catalytic reduction (SCR) or lean NO_x traps (LNT). Both of these techniques will require on-board NO_x sensors, to control either reagent injection (SCR) or trap regeneration (LNT). Broadly speaking, a suitable NO_x sensor for these applications would be operative at temperatures near 600 °C and able to measure [NO_x] in the concentration range 10–1000 ppm_V [2,3].

It is important to realize that at these elevated temperatures (~600 °C) the dominant equilibrium NO_x species is the monoxide (NO) [4], and thus the focus of this work is to develop sensing elements that can respond to NO at temperatures near 600 °C. The technique employed is "biasing", in which a dc electrical signal is applied to the sensing element. This technique has previously been employed for NO_x sensing by Ho et al. [5], who applied DC voltages to a sensing element consisting of Nd_2CuO_4 and Pt electrodes on opposite sides of a yttria-stabilized zirconia (YSZ) disk. The presence of NO_x produced an increase in DC current (*I*) at 400 °C. DC voltage biasing of elements similar to those described by Ho et al. was also reported by Grilli et al. [6], except the oxide electrode was $LaFeO_3$ and testing was carried out at 450 °C.

Miura et al. [7] applied DC voltages (in the range 0.1–0.5 V) to YSZ-based sensing elements consisting of one Pt electrode and one $CdCr_2O_4$-coated Pt electrode. Two designs were presented, the first was a tubular design in which only the $CdCr_2O_4$-coated electrode was exposed to the NO_x-containing gas. In the second design, the electrodes were co-planar and both were exposed to the NO_x. The DC current between the electrodes was shown to be proportional to [NO_x] for both designs, and the tubular design could be biased to a "NO-selective" condition at 500 °C.

In this study we are attempting to extend and build upon this prior work by increasing the operating temperature above

* Corresponding author. Tel.: +1 865 576 2264; fax: +1 865 574 4357.
E-mail address: westdl@ornl.gov (D.L. West).

0925-4005/$ – see front matter © 2005 Elsevier B.V. All rights reserved.
doi:10.1016/j.snb.2005.06.043

500 °C, and systematically examining the effects of varying both electrode materials and electrode geometry. We also explore the use of constant current (as opposed to constant voltage) biasing, and focus on sensing elements with co-planar electrodes.

2. Experimental procedure

The geometries of the sensing elements prepared for the present investigation are shown in Fig. 1a. All geometries consisted of co-planar oxide and Pt electrodes on a YSZ substrate. Most of the sensing elements prepared had the "semicircular" (SC) geometry, the other two geometries ("interdigitated" (ID) and "asymmetric" (AS)) were considered

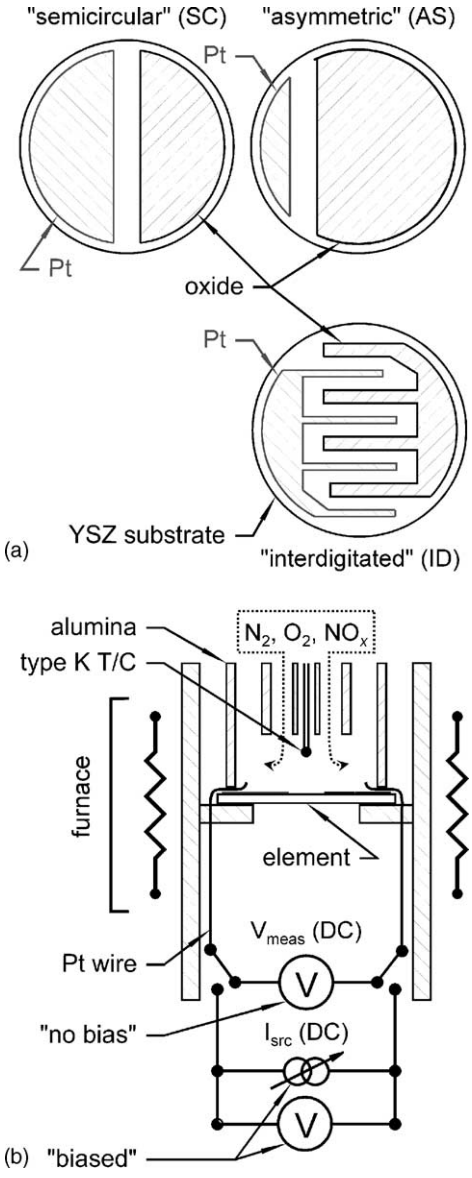

Fig. 1. Schematic view of sensing element geometries (a) and the test apparatus for evaluating NO_x sensing performance (b).

Table 1
Electrode materials and firing conditions

Material	Vendor	Firing T, t (°C, h)
Pt	Electroscience	1100, 0.3
NiO	J.T. Baker	1100, 1.0
ZnO	Alfa Aesar	1100, 1.0
$La_{0.80}Sr_{0.20}FeO_{3-\delta}$ (LSF)	Praxair	900, 1.0
$La_{0.85}Sr_{0.15}CrO_3$ (LSC)	Praxair	900, 1.0
$La_{0.85}Ba_{0.15}CrO_3$ (LBC)	Praxair	900, 1.0

variations on the SC geometry with approximately the same total area. The YSZ (8 mol% Y_2O_3, Tosoh) substrate was produced by tape casting, laminating, and sintering (1400 °C, 2 h, air) to produce disks about 16 mm in diameter and 1 mm in thickness. The electrodes were applied by first screen printing and firing (1100 °C, 0.3 h, air) the Pt (Electroscience) electrode and then screen printing and firing the oxide electrode for one hr. in air. The Pt was obtained as a dispersion ready for screen printing and the screen-printing dispersions for the oxides were produced in-house.

Several different oxides were employed as electrode materials, and these are listed in Table 1. These were selected either for their reported usefulness as semiconducting gas sensor materials (ZnO and NiO [8]), or materials with high electrical conductivity (LSF, LSC and LBC [9]). The firing temperatures of the oxide electrodes are listed in Table 1, it can be seen there that the perovskite (LSC, LBC, and LSF) electrodes were fired at lower temperature than the binary oxide (NiO and ZnO) electrodes. This was done in order to avoid reaction between the La-containing perovskites and the YSZ, as described by Yamamoto et al. [10].

Fig. 1b shows schematically the apparatus used to characterize NO_x sensing performance. The elements were placed, centrally located, in a resistively heated furnace and pressure contacts to the elements were made with Pt wire. An Environics 4000 gas mixing unit (not shown in Fig. 1b) was used to mix N_2, O_2, and NO_x (5000 ppm NO or NO_2 in N_2) and these mixtures were presented to the electroded side of the sensing elements at a flow rate of 0.75 l/min. A type K thermocouple was placed approximately 1 cm from the electroded element surface and was used to monitor the sensing element temperature. The temperature indicated by this thermocouple typically was about 3–5° lower than that indicated by the furnace control thermocouple, which was located just outside the resistive heating elements of the furnace. As indicated in Fig. 1b, voltage measurements were made both with and without bias. For measurements without bias, a Keithley 617 electrometer was used to measure the DC voltage developed across the element electrodes, and for measurements with bias, a Keithley 2400 source meter was placed in parallel with the electrometer.

Primarily, two types of NO_x sensing performance evaluations were carried out, both at constant temperature and a constant $[O_2]$ of 7 vol.%. In the first type, intended to gauge the effect of different current biases on the NO_x response of the elements, the bias was stepped at discrete levels (e.g.,

−16, −8, 0, 8, 16 μA for 5 min each) and a brief (2 min) 450 ppm_V pulse of either NO or NO_2 was applied at each bias level. This enabled a rapid assessment of the changes induced in the measured voltage by NO or NO_2 at different current bias levels. In the second type of test, the current bias was set at a fixed level (some tests were carried out with no bias, and we consider this to be a case of fixed bias with $I_{bias} = 0.0$), and the input [NO_x] (either NO or NO_2) was varied systematically between 20 and 1500 ppm_V.

Subsequent to evaluation of NO_x sensing performance, the elements were carbon-coated in an evaporator and the surface microstructure examined with an SEM (Hitachi S-800, 5 kV accelerating voltage, secondary electron mode). Elements were also cross-sectioned, polished, and examined with light optical microscopy in order to gain a measure of the fired electrode thickness.

3. Results and discussion

3.1. Electrode microstructure

Fig. 2 shows plan views of the electrode microstructures post-test. All the electrodes appear porous, which should be a desirable characteristic for gas sensing. The Pt electrode seems to feature a bimodal particle size distribution, while all the oxides except the $La_{0.80}Sr_{0.20}FeO_{3-\delta}$ (LSF) appear to consist of a narrower range of particle sizes. The ZnO and LSF electrodes contain primarily sintered agglomerates but the agglomerates consist of coarser primary particles in the ZnO electrode. The two chromite electrodes ($La_{0.85}Sr_{0.15}CrO_3$ (LSC) and $La_{0.85}Ba_{0.15}CrO_3$ (LBC)) appear very similar to each other, and do not display the distinct faceting observed in the NiO electrode. Cross-sectioning and metallographic examination indicated that typical electrode thicknesses were about 20 μm for the Pt electrodes and about 30 μm for the oxide electrodes.

3.2. Sensing performance without bias

Some typical results of the sensing performance observed without current bias are shown in Fig. 3. The elements responded very strongly to NO_2, and over the range 20–200 ppm_V the response was well described by a logarithmic expression. All the oxides in Table 1 (which include both n (ZnO [11]) and p (e.g., LSC [9]) type) yielded the same algebraic sign for the NO_2 response. This differs from the behavior reported by Di Bartolomeo et al. [12], who tested sensing elements made with two co-planar interdigitated Pt electrodes, one of which was partially covered with an oxide. WO_3 (an n-type oxide) and LSF (a p-type oxide) were reported to yield NO_2 responses of different sign, and this was attributed to a "differential electrode equilibria" sensing mechanism. Whether the differences in element geometry employed here and by Di Bartolomeo et al. account for the differing observations remains to be resolved.

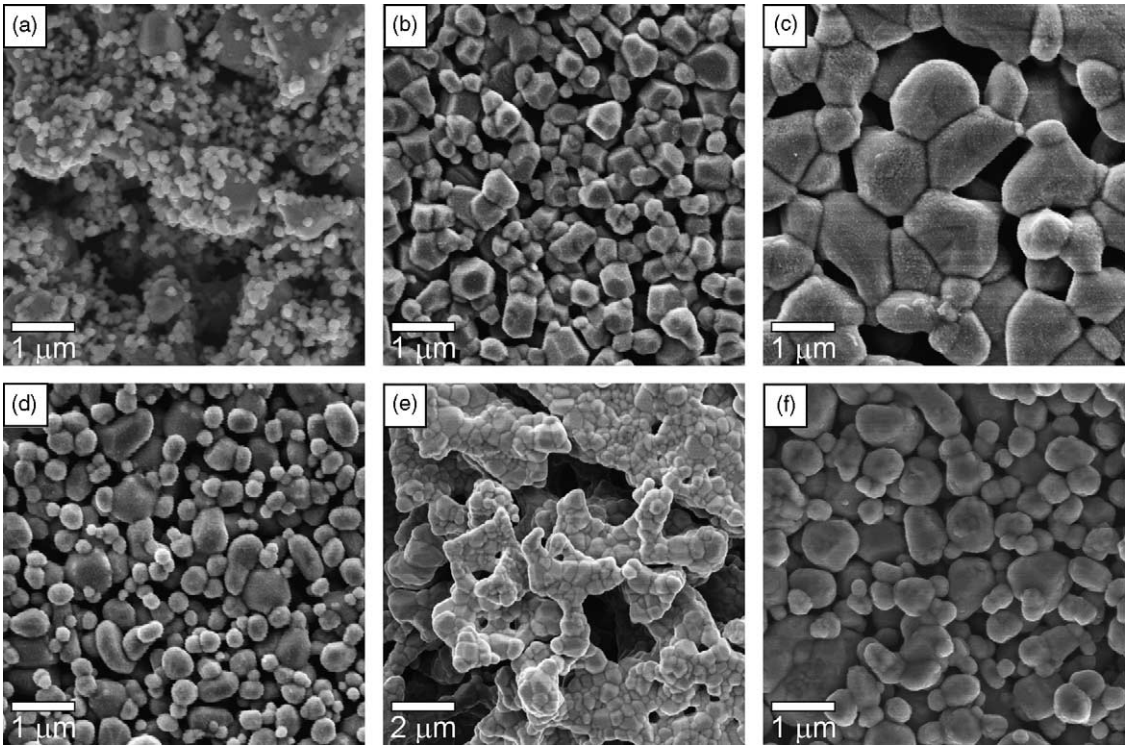

Fig. 2. Electrode microstructures in plan view is: (a) Pt, (b) NiO, (c) ZnO, (d) $La_{0.85}Ba_{0.15}CrO_3$ (LSC), (e) $La_{0.80}Sr_{0.20}FeO_{3-\delta}$ (LSF), and (f) $La_{0.85}Sra_{0.15}CrO_3$ (LSC). Secondary electron images at 5 kV accelerating voltage, Hitachi S-800.

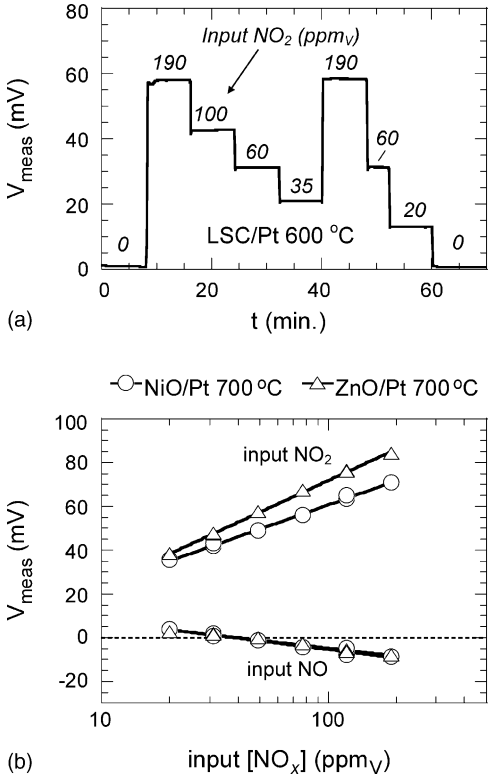

Fig. 3. NO_x sensing performance with no bias current shows: (a) the measured voltage as the input [NO_2] was varied (600 °C, 7 vol.% O_2) with a sensing element constructed using LSC and Pt (semicircular geometry); (b) the measured voltages as a function of [NO_x] for semicircular sensing elements using ZnO and NiO with Pt at 700 °C (also 7 vol.% O_2). The lines drawn are logarithmic fits.

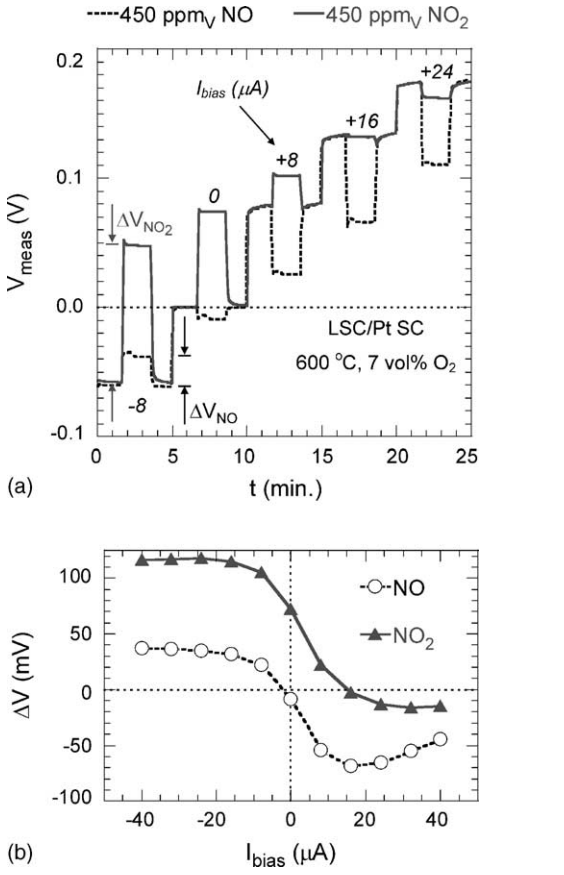

Fig. 4. Measured voltages during pulses of 450 ppm_V NO_x at different bias current levels (a) and the computed changes in voltage due to 450 ppm_V NO_x as a function of current bias (b). The method of estimating the voltage changes due to the NO_x (ΔV_{NO_2} and ΔV_{NO}) plotted in (b) are shown in (a).

As seen in Fig. 3b, the sensing response to NO was much weaker (and opposite in sign) than that to NO_2, and this is in agreement with observations by other workers on non-Nernstian solid-electrolyte NO_x sensing elements [3]. Thus, employment of these sensing elements for exhausts at temperatures near 600 °C (a temperature at which much of the NO_x is predicted to be NO) would require either a mechanism for conversion of the NO_x to NO_2 as described by Kunimoto et al. [13] or equilibration of the NO_x-containing mixture at a temperature below that of the sensing element as described by Szabo and Dutta [14]. The approach adopted here was to employ DC electrical biasing to enhance the NO response, as detailed in the immediately following section.

3.3. Effect of electrical biasing on the NO_x response

Fig. 4a shows the measured voltage (with a LSC/Pt sensing element, semicircular geometry, 600 °C, 7 vol.% O_2) during 450 ppm_V pulses of NO_x at different current biases, and Fig. 4b shows the derived changes in voltage (ΔV, computed as indicated in Fig. 4a) due to 450 ppm_V NO_2 for this sensing element over the bias range −40 to 40 μA. At negative biases (negative bias corresponding to the oxide electrode in Fig. 1a being biased negatively with respect to the Pt electrode), the introduction of 450 ppm_V NO_2 causes a large positive change (ΔV_{NO_2}) in V_{meas}, whereas 450 ppm_V NO causes a smaller positive change (ΔV_{NO}). With no or small positive current bias, ΔV_{NO_2} is positive and ΔV_{NO} is negative. As the current bias is increased further, ΔV_{NO_2} is eventually driven to zero (at ∼16 μA) and at higher positive biases both ΔV_{NO_2} and ΔV_{NO} are negative.

The behavior observed in Fig. 4 can be *partially* rationalized by considering that first, the current source will vary the output voltage to keep the dc current constant, and second, that the current carrying species in the Pt wire are electrons and in the YSZ substrate the current carrying species are oxygen ions. Fig. 5 shows schematically the direction of travel for each of these species under conditions of both negative and forward bias. With negative bias, in order for current to flow, one or more of the following oxidation reactions must take place at the Pt electrode:

$$NO + O^{2-} \rightarrow NO_2 + 2e^- \quad (1)$$

or

$$O^{2-} \rightarrow \tfrac{1}{2}O_2 + 2e^- \quad (2)$$

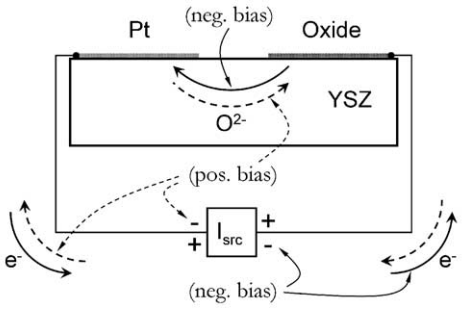

Fig. 5. Schematic of current flow in a biased sensing element. O^{2-} represents an oxygen ion in the YSZ substrate.

Similarly, for current to flow with negative bias one or more of the following reduction reactions must take place at the oxide electrode:

$$NO + 2e^- \rightarrow \tfrac{1}{2}N_2 + O^{2-} \quad (3)$$

or

$$NO_2 + 2e^- \rightarrow NO + O^{2-} \quad (4)$$

or

$$\tfrac{1}{2}O_2 + 2e^- \rightarrow O^{2-} \quad (5)$$

In Eqs. (1)–(5) all molecular species are gaseous and O^{2-} represents an oxygen ion in the YSZ solid electrolyte.

Referring to Fig. 4b, the introduction of 450 ppm NO or NO_2 causes a decrease in $|V_{meas}|$ at negative bias, indicating that the apparent element resistance has decreased (as less voltage is required to maintain the current). With negative bias, NO can be oxidized (via Eq. (1)) at the Pt electrode and NO_2 can be reduced (via Eq. (4)) at the oxide electrode. This will effectively lower the resistance of the sensing element and thus lead to a decrease in the magnitude of the voltage ($|V_{meas}|$) required to maintain a given current. Similar considerations regarding oxidation of NO at the oxide electrode may account for the consistent decrease in V_{meas} with NO that is seen at positive biases in Fig. 4, and the decrease seen with NO_2 at sufficiently large current biases (>16 μA) may be due to reduction of this species at the Pt electrode.

The behavior observed with NO_2 at smaller negative and positive biases in Fig. 4 is more difficult to explain. First considering the small negative bias regime, Fig. 4a indicates that in the presence of 450 ppm_V NO_2 an applied voltage of ∼+50 mV is required to maintain a current of −8 μA. This could be interpreted as the current source having to "work against" the voltage generated by the presence of NO_2. (As shown in Fig. 3a, with no bias current, NO_2 induces a positive voltage on the LSC electrode relative to the Pt electrode, and Fig. 4 shows that this voltage is about 75 mV with 450 ppm_V NO_2.) This interpretation is difficult to verify as it requires one to compare the voltage measured with no current flowing to the voltage measured with −8 μA of current. The increase in V_{meas} seen with 450 ppm_V NO_2 at +8 μA bias is similarly difficult to explain, as is the fact that at +16 μA the introduction of NO_2 causes little change in V_{meas}.

Although the details of the mechanism are not as yet fully understood, the data in Fig. 4 indicate that at approximately 16 μA bias the sensing element does not respond strongly to 450 ppm_V NO_2 but responds strongly to 450 ppm_V NO. Thus, it is "NO-selective", and as Fig. 6 shows this "selectivity" was preserved (at 14 μA bias) over a wide concentration range, from 1500 ppm_V NO_x down to concentrations on the order of 50 ppm_V (it can be seen in Fig. 6 that at low [NO_x] (<∼50 ppm_V) the response to NO_2 is becoming commensurate with that to NO). Therefore, DC-biased sensing elements of the type described here could be useful in situations where it is desired to measure [NO] in NO_x-containing mixtures of unknown [NO]/[NO_2], or in sensor designs where the NO_x mixture is equilibrated at a high temperature such that NO is dominant.

3.4. Effect of electrode materials and geometry

Testing of the type illustrated in Fig. 4 (at either 600 or 700 °C) was conducted with sensing elements made from all the oxides in Table 1 (semicircular geometry, paired with Pt).

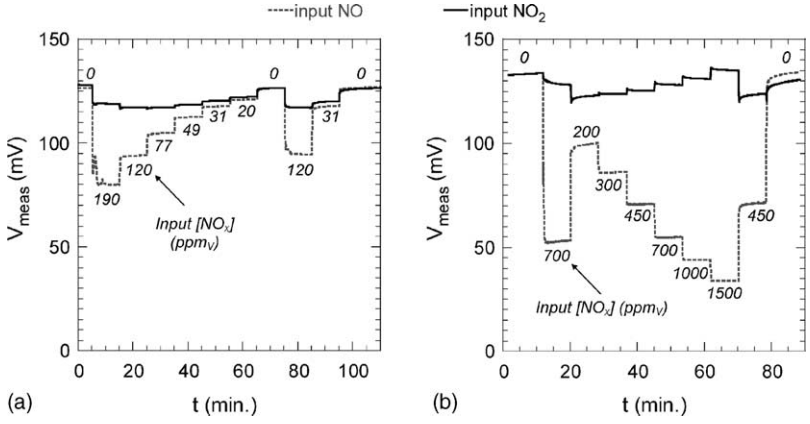

Fig. 6. Measured voltage during [NO_x] variations at 600 °C for a LSC/Pt sense element (semicircular geometry) with +14 μA current bias. Data collected in 7 vol.% O_2.

Of these materials, only LBC displayed behavior quantitatively similar to that shown in Fig. 4, and the response of this material (on a percentage basis relative to the background) was only about half of that displayed by LSC. For the other oxides the behavior varied considerably from that shown in Fig. 4b. ZnO and NiO produced a very large response to NO_2 at negative bias (particularly NiO), but this response could not be driven to zero at positive bias as was the case for LSC and LBC, and the response to NO generally was weak. The element prepared with LSF displayed very interesting behavior, featuring a large positive response to NO_2 and a large negative response to NO at positive bias. Since the focus of the investigation was optimizing the NO response of the sensing elements, further study was confined to the materials combination that produced the best NO response (LSC and Pt).

To study the effects of electrode geometry, elements with the two "variant" geometries shown in Fig. 1a (interdigitated (ID) and asymmetric (AS)) were constructed using LSC and Pt. Similar testing as shown in Fig. 4 was carried out to identify the bias level for "NO-selectivity" at 600 °C, 7 vol.% O_2, and 450 ppm_V NO_x (this differed for the two sensing elements). The bias was then fixed at this level and the input [NO] varied systematically as was done during the generation of the data shown in Fig. 6b. The changes in voltage due to NO (plotted as the percent change from the voltage with 0 ppm_V NO) are shown in Fig. 7. It can be seen there that the geometry changes did not appear to dramatically affect the functional form of the ΔV versus NO_x characteristic, but there is perhaps some diminution of response with the "asymmetric" geometry. The tentative conclusion drawn was that the sensing element response magnitude was not strongly affected by adopting the variant geometries depicted in Fig. 1a.

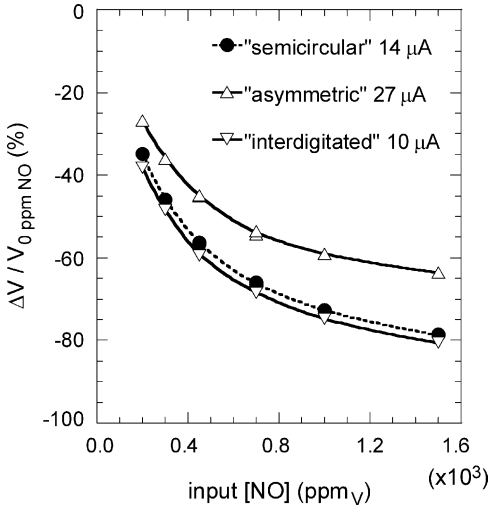

Fig. 7. Changes in voltage due to NO for LSC/Pt sense elements with each of the geometries shown in Fig. 1a. The bias current during the measurements is given in the legend. Data collected at 600 °C and in 7 vol.% O_2.

3.5. Effects of temperature

In order to study the effect of temperature on sensing performance testing as illustrated in Fig. 4 was carried out on the LSC/Pt semicircular element at 500 and 700 °C. The current bias for "NO-selectivity" was determined to be 1.5 and 60 μA at 500 and 700 °C, respectively. Fig. 8a shows how the measured voltage varied with input [NO] with the "NO-selective" bias at each of these temperatures, along with the data that was presented earlier in Fig. 6a. Increasing the temperature drastically reduces the response to NO, which is unfortunate for the intended application but is consistent with the supposition made earlier that the sensing response to NO involves oxidation of this species to NO_2. This oxidation should become more difficult as the temperature increases above 500 °C.

Fig. 8b shows that as [NO] decreases, the ΔV versus [NO] characteristic displays a linear regime, the extent of which decreases with decreasing T. This behavior, combined with the observation earlier that at low NO_x the response to NO_2 was commensurate with that to NO (when 450 ppm_V NO_x was used to estimate the bias for "NO-selectivity"), could have ramifications for the use of these types of sensing ele-

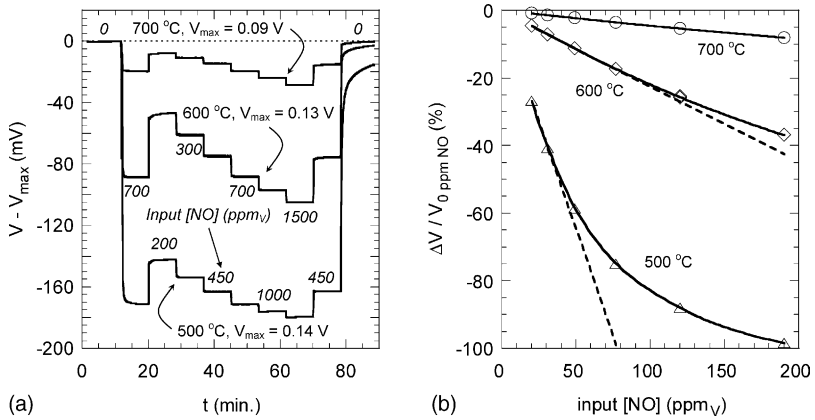

Fig. 8. (a) Measured voltages during [NO] variations at 500, 600, and 700 °C for a LSC/Pt sense element (semicircular geometry) current-biased to "NO-selective". (b) The computed changes in V_{meas} due to NO for 20 $ppm_V \leq [NO] \leq 190$ ppm_V at these same temperatures. Data collected in 7 vol.% O_2.

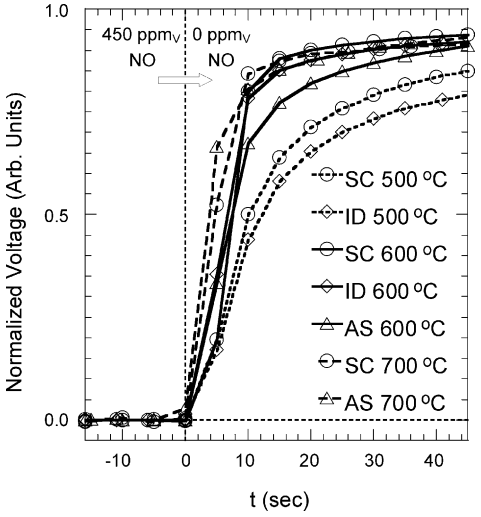

Fig. 9. Recovery from exposure to 450 ppm NO for sensing elements with the geometries shown in Fig. 1a. Data collected in 7 vol.% O_2.

ments at low NO_x levels. Finally, it can be seen from Fig. 8a that the recovery from 450 ppm_V NO exposure is much more sluggish at 500 °C than at 700 °C. In order to investigate whether the sample geometry had any effect on this behavior, the recovery from 450 ppm_V NO was examined at various temperatures for each of the element geometries in Fig. 1a. As shown in Fig. 9, there did not appear to be any systematic effect of electrode geometry on the recovery behavior. This combined with the observations presented earlier led to the conclusion that the simple geometry variations in Fig. 1a had minimal impact on the response characteristics of the sensing elements prepared for the present investigation.

4. Conclusions

Use of DC current biasing enabled "NO-selective" sensing behavior at ~600 °C for YSZ-based sensing elements with co-planar oxide and Pt electrodes if the oxide was an alkaline-earth modified lanthanum chromite. Proper selection of the current bias led to selective enhancement of the NO response (relative to the NO_2 response) over a wide range of [NO_x], from ~50 ppm_V to 1500 ppm_V. The effect was not observed in another alkaline-earth modified lanthanum perovskite ($La_{0.8}Sr_{0.2}FeO_{3-\delta}$) nor in the binary oxides NiO and ZnO. Operating temperature had a strong effect on the NO sensing performance, with higher temperatures leading to a diminished response magnitude but a shorter recovery time from NO exposure. The observations suggest that DC current-biased sensing elements using alkaline-earth modified lanthanum chromite and Pt electrodes may be useful for NO sensing at temperatures near 600 °C.

References

[1] J.T. Woestman, E.M. Logothetis, Controlling automotive emissions, Ind. Phys. 1 (1995) 21–24.
[2] F. Menil, V. Coillard, C. Lucat, Critical review of nitrogen monoxide sensors for exhaust gases of lean burn gasoline engines, Sens. Actuators B: Chem. 67 (2000) 1–23.
[3] N. Miura, M. Nakatou, S. Zhuiykov, Impedancemetric gas sensor based on solid electrolyte and oxide sensing electrode for detecting total NO_x at high temperature, Sens. Actuators B: Chem. 93 (2003) 221–228.
[4] K.B.J. Schnelle, C.A. Brown, Air Pollution Control Technology Handbook, CRC Press, Boca Raton, 2001.
[5] K.-Y. Ho, M. Miyayama, H. Yanagida, NOx response properties in dc current of Nd_2CuO_4/4YSZ/Pt element, J. Ceram. Soc. Jpn. 104 (1996) 995–999.
[6] M.L. Grilli, E. Di Bartolomeo, E. Traversa, Electrochemical NO_x sensor based on interfacing nanosized $LaFeO_3$ perovskite-type oxide and ionic conductors, J. Electrochem. Soc. 148 (2001) H98–H102.
[7] N. Miura, G. Lu, M. Ono, N. Yamazoe, Selective detection of NO by using an amperometric sensor based on stabilized zirconia and oxide electrode, Solid State Ionics 117 (1999) 283–290.
[8] T. Seiyama, S. Kagawa, Study on a detector for gaseous components using semiconductive thin films, Anal. Chem. 38 (1966) 1069–1073.
[9] A.J. Moulson, J.M. Herbert, Electroceramics, Chapman and Hall, London, 1990, pp. 122–123.
[10] O. Yamamoto, Y. Takeda, R. Kanno, M. Noda, Perovskite-type oxides as oxygen electrolytes for high temperature oxide fuel cells, Solid State Ionics 22 (1987) 241–246.
[11] S.P. Pearton, D.P. Norton, K. Ip, Y.W. Heo, T. Steiner, Recent progress in processing and properties of ZnO, Prog. Mater. Sci. 50 (2005) 293–340.
[12] E. Di Bartolomeo, M.L. Grilli, E. Traversa, Sensing mechanism of potentiometric gas sensors based on stabilized zirconia with oxide electrodes, J. Electrochem. Soc. 151 (2004) H133–H139.
[13] A. Kunimoto, M. Hasei, Y. Yan, Y. Gao, T. Ono, Y. Nakanouchi, New total-NO_x sensor based on mixed potential for automobiles, SAE Tech. Pap. Ser. 1999-01-1280, 1999.
[14] N.F. Szabo, P.F. Dutta, Strategies for total NO_x measurement with minimal CO interference utilizing a microporous zeolitic catalytic filter, Sens. Actuators B: Chem. 88 (2002) 168–177.

Biographies

Dave West is a post-doctoral research associate at Oak Ridge National Laboratory (ORNL). He received a BA in Physics from the University of California in 1987 and MS and PhD degrees, both in materials science and engineering, from the University of Washington (MS, 1996) and the University of Illinois (PhD, 2002).

Fred Montgomery is a senior staff scientist at ORNL, and holds BS and PhD degrees in chemistry from the University of Oregon (BS, 1966) and the University of Rochester (PhD, 1971).

Tim Armstrong is the ORNL hydrogen, fuel cell, and infrastructure manager. He received a BS in ceramic engineering from The Ohio State University (1984) and a PhD, also in ceramic engineering, from the University of Illinois (1989).